Engineering Fracture Mechanics 219 (2019) 106641

Contents lists available at ScienceDirect

Engineering Fracture Mechanics

journal homepage: www.elsevier.com/locate/engfracmech

Hydrogen enhanced fatigue crack growth rates in a ferritic Fe-3 wt %Si alloy and a X70 pipeline steel

Antonio Alvaro[a,b,*], Di Wan[b], Vigdis Olden[a], Afrooz Barnoush[b]

[a] SINTEF Industry, Dept. of Materials Integrity and Welding, 7456 Trondheim, Norway
[b] Department of Mechanical and Industrial Engineering, Norwegian University of Science and Technology, 7491 Trondheim, Norway

ARTICLE INFO

Keywords:
Hydrogen embrittlement
Fatigue crack growth
Steel

ABSTRACT

It is well known that ferrous materials can be damaged by absorption of hydrogen. If a sufficient quantity of hydrogen penetrates into the material, static fracture and the material's fatigue performances can be affected negatively, in particular causing an increase in the material crack growth rates. The latter is often referred as Hydrogen Affected-Fatigue Crack Growth Rate (HA-FCGR). It is therefore of paramount importance to quantify the impact, in terms of hydrogen induce fatigue crack growth acceleration in order to determine the life of components exposed to hydrogen and avoid unexpected catastrophic failures. In this study, in-situ fatigue crack growth rate testing on Compact Tension (CT) specimens were carried out to determine the fatigue crack growth behaviour for a Fe-3 wt%Si alloy and X70 pipeline steel. Tests were carried out in two environmental conditions, i.e. laboratory air and in-situ electrochemically charged hydrogen, and different mechanical conditions in terms of load ratio (R = 0.1 and R = 0.5, for the Fe-3 wt% Si, R = 0.1 for the X70 steel) and test frequency (f = 0.1 Hz, 1 Hz and 10 Hz) were adopted under electrochemically charged hydrogen conditions. The results show a clear detrimental effect of H for the specimens tested in hydrogen when compared to the specimens tested in air for both materials and that the impact of hydrogen is test frequency-dependent: the hydrogen induced acceleration is more prominent as the frequency is decreased. Post-mortem surface investigations consistently relate the global crack growth acceleration to a shift from transgranular to Quasi-cleavage fracture mechanism. Despite such consistency, the acceleration factor strongly depends on the material: Fe-3wt%Si features acceleration up to 1000 times while X70 accelerates up to 76 times when compare to the material fatigue crack growth rate recorded in air. Observation of the deformation activities in the crack wake in relation to the transition into hydrogen accelerated regime in fatigue crack growth show a tendency toward restricted plastic activity in presence of hydrogen.

1. Introduction

It is well established that the presence of atomic hydrogen affects the fatigue behavior in ferrous materials under cyclic stresses. It is of important significance for both the new and the long-standing applications in industries which operate in aggressive environments involving hydrogen. The understanding of the basic mechanisms underlying hydrogen induced degradation phenomena as well as their macroscopic quantification is vital in order to avoid failures which may have negative impact for the environment, determine industrial economical loss and, in the worst cases, jeopardize personnel health. Therefore, the development of the knowledge of the

* Corresponding author.
E-mail address: antonio.alvaro@sintef.no (A. Alvaro).

https://doi.org/10.1016/j.engfracmech.2019.106641
Received 21 April 2019; Received in revised form 20 August 2019; Accepted 21 August 2019
Available online 29 August 2019

mechanical behavior of metallic materials when directly in contact with hydrogen is strongly connected to a quantitative evaluation of the hydrogen influence on mechanical properties of steels which is necessary for a suitable and proper design of hydrogen-contact prone components and structures. On the other hand, such information is of paramount importance when it comes to maintenance strategies and decision about inspection periods: platforms, umbilicals, risers, flowlines and subsea pipelines, which are continuously subjected to oscillatory environmental loads and, at the same time, to hydrogen uptake from cathodic protection or H_2S containing fluids [1,2]. Degradation by hydrogen under such conditions would manifest as a reduced resistance to fatigue crack growth. Failures during operation in which hydrogen has played an important role, are however difficult to be discerned from the hydrogen-free failures, due to the volatile nature of the hydrogen atom. Worldwide, it is generally considered that over 80% of all service failures can be related to mechanical fatigue [3]. In design of offshore structures, the determination of the remaining life of a given component is based on the knowledge of the critical defect size and the crack growth rate. The understanding and the quantitative determination of the effect of hydrogen on the crack growth rate is therefore of paramount importance for a reliable design and life extension of oil and gas fields: the loading condition may be modified or inspection periods arranged so that the crack is detected before failure [4].

The typical material crack growth rate behavior is usually described by means of the ΔK- da/dN plots on which three main domains can be distinguished: stage I (threshold domain), stage II (Linear or Paris domain) and stage III (final fracture). Since the stage III is related to the unstable crack growth and the final failure, it is often considered of least importance. However, both the stage I and in particular the stage II, also commonly known as Paris domain, can be to different degrees affected by the presence of hydrogen. The challenge in univocally determine the impact of atomic hydrogen on the crack growth properties of a material is due to the fact that it is highly dependent on several and often interacting factors: the material system, the load frequency, the load ratio, temperature, pressure (in the case of H_2 pressurized gas application) or cathodic potential level (for application where cathodic protection is needed). Understanding the nature and quantifying the magnitude of hydrogen-induced acceleration of fatigue crack growth rate is necessary in order to assess the eligibility of material in applications where hydrogen uptake into the material is a real possibility when it comes to fatigue life design. In this work, the HA-FCGR of two iron-based materials have been studied: a Fe-3 wt% Si alloy with coarse grain size as a model material and a commercial X70 pipeline steel as a case study. The Fe-3 wt%Si model material was designed with the intent to provide a clean ferritic “canvas” to obtain fundamental insights into a “pure” hydrogen-material interaction while the X70 pipeline steel was investigated as verification toward material of everyday use in practical applications. The coarse grain size of the model material can avoid some complexities rising from the interfaces and can make the data analysis and interpretation much simplified and more straightforward. It has been shown that Fe-3 wt%Si alloy features an acceleration in the HA-FCGR by up to 1000 times under cathodic charging condition in comparison with the reference test in lab air, while the X70 pipeline steel accelerates up to 76 times in the HA-FCGR. This work can shed some light on the mechanistic discussion on the HA-FCGR and this can be verified by the case study on the X70 pipeline steel.

2. Methods

2.1. Materials

The alloys included in this study are Fe-3 wt%Si with a pure ferritic microstructure and a commercial X70 pipeline steel with a ferritic-pearlitic microstructure. The detailed chemical compositions are given in Table 1 and the microstructures in Fig. 1.

In order to obtain the most equiaxed grain as possible for the Fe-3 wt%Si materials, the raw plates were obtained by hot rolling followed by 10% cold rolling plus annealing at 800 °C for three times with the last annealing temperature of 1050 °C before the final straightening. The average grain size was of about 300 μm, as shown in Fig. 1. The yield strength ($R_{p0.2}$) and the ultimate tensile strength (R_m) were 485 MPa and 555 MPa, respectively.

For the X70 material the samples were taken from the longitudinal direction of a pipe with a wall thickness of 23.3 mm. The yield ($R_{p0.2}$) and ultimate tensile strength (R_m) are 485 MPa and 600 MPa, respectively. As shown in Fig. 1, the X70 microstructure is mainly banded ferrite-pearlite (the white phase is ferrite and the darker phase is pearlite). The average grain size is 30 μm.

2.2. Fatigue crack growth rate testing

Fatigue crack growth rate testing was performed on Compact Tension (CT) specimens (in accordance with the dimensions recommended in ASTM E647 standard, see Fig. 2), which were cut by electron discharge machining (EDM) from the raw materials.

The FCGR tests were carried out in air and in in-situ electrochemical charging conditions at room temperature. The test specimens were in-situ cathodically charged in a 0.1 M Na_2SO_4 electrolyte with a constant potential of $-14001\ mV_{SCE}$. Multimeters were used during the whole test in order to check the values and keep the circuit run as designed.

Table 1
Chemical composition of Fe3%Si alloy and X70 pipeline steels used in this work.

Element	C	Si	Mn	P	S	Cu	Ni	Fe
Fe3%Si [wt%]	0.018	3.0	0.055	0.008	0.003	0.013	0.006	Balance
X70 [wt%]	0.090	0.3	0.710	0.010	0.001	0.300	0.250	Balance

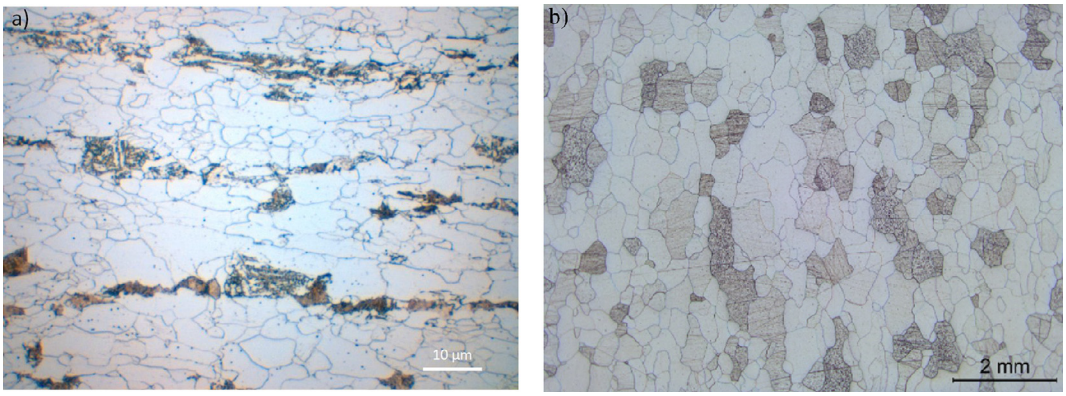

Fig. 1. Microstructures of the investigated material: (a) X70 where the white phase is ferrite and the darker phase is pearlite; (b) Fe-3 wt%Si constituted by coarse grained ferrite. The darker appearance of some of the grains is due to their slightly different response to etching.

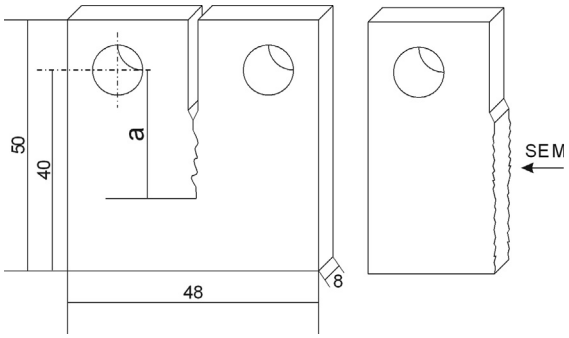

Fig. 2. Geometry and main dimensions of the Compact Tension specimen used for testing and schematic representation of the fracture surface investigation.

Before testing, the specimens were fatigue pre-cracked according to the procedure described in [5]. First, a lower bound threshold stress intensity factor range between 10 and 12 MPa·m$^{0.5}$ was used to initiate the crack from the notch. Then a reduction in the ΔK value of 5% was adopted stepwise until the target K-value was reached, and the crack growth stabilized. Typically, these pre-cracks were in the range of 2–4 mm after approximately 200,000 cycles for these materials. It should be noted that the crack front is not necessarily a straight line after pre-cracking: the start/stop reference crack length is estimated as an average from of nine points from the crack front equally distributed across the specimen thickness. A 5% increase in the ΔK from the last step of the pre-cracking procedure was used to get the crack growing and in order to minimize the effect of the plastic zone from the pre-cracking procedure. Alternate current-potential drop (AC-PD) crack growth rate measure box was used during the test to record the crack length and derive the FCG rate behavior. After testing, the specimens were broken up in liquid nitrogen and the da/dN vs ΔK curves were obtained from start/stop crack length measurements.

Testing in air was performed at 10 Hz and at two load ratios, i.e. R = 0.1 and 0.5 for the Fe-3 wt%Si and R = 0.1 for X70 steel. In-situ cathodically charged FCG tests were carried out at three different frequencies, 0.1 Hz, 1 Hz and 10 Hz and applying a carefully designed environmental chamber mounted to the test rig (see Fig. 3). The same load ratios as for the tests in air were applied.

2.3. Post-mortem characterization

Post-mortem fractographic characterization was performed on all the tested specimens using a Scanning Electron Microscope (SEM). The FEG Quanta 650 environmental SEM (Thermo Fisher Scientific Inc., USA) was operated at 20 kV acceleration voltage with an aperture size of 50 µm while the quantitative information obtained from the fracture surfaces were done by using the built-in software on the cross section of the specimen as shown in the schematic reported in Fig. 2.

3. Results

3.1. Fatigue crack growth rates

Fatigue crack growth rate tests on Fe-3 wt%Si were performed in air (10 Hz) and in-situ under electrochemical hydrogen charging (load ratios of 0.1 and 0.5 and frequencies of 0.1, 1 and 10 Hz. The stage II fatigue crack growth domain was quantitively described

Fig. 3. Set-up of the test rig for in-situ electrochemically charged fatigue crack growth rate test, with close up photos of testing performed in air and in in-situ electrochemical charging conditions.

through the Paris law [6]:

$$da/dN = C \cdot \Delta K^m \tag{1}$$

where a is the crack length and N is the number of the cycles, giving da/dN the discrete crack extension/growth per cycle. C and m on the right-hand side of the equation are constants that depend on the material and the testing conditions, while ΔK is the range of the stress intensity factor experienced by the material during the fatigue cycles.

The resulting FCG rate curves are shown in Fig. 4 while the derived Paris constants C and m are summarized in Table 2.

The specimens tested under H-charging conditions generally exhibited a higher FCGR than the one tested in air. The hydrogen induced crack growth rate acceleration shows a strong dependency with respect to the test frequency: the lower the frequency, the more pronounced is global crack growth rate acceleration. The Paris' law parameters obtained from the curves and summarized in the table in Fig. 4 show that: the presence of hydrogen induces an acceleration in crack growth of about 1000 times compared to testing in air. The low variation in m values indicates a minor shift in the curves slope, i.e. the effect of hydrogen is independent on the ΔK level in the Paris' domain. The effect of the load ratio is also consistent: except for the test performed at 10 Hz for which little to none hydrogen influence is registered. All the test performed at R = 0.5 featured a higher crack growth rate acceleration than the ones recorded at R = 0.1.

Similarly as reported for the Fe-3 wt%Si, the resulting FCG rate curves for the X70 pipeline steel are shown in Fig. 5 together with a table summarizing the Paris constants C and m.

Contrarily to the behaviour exhibited by Fe-3 wt%Si, the X70 steel showed a generally lower acceleration factor (about 76 times for test performed at 0.1 Hz, against 500 times for the same conditions for Fe-3 wt%Si) and a clear ΔK-value for the onset of HA-FCG for the test performed at 1 Hz. On the other hand, also for the X70 steel, a low variation in the Paris constant m is recorded overall.

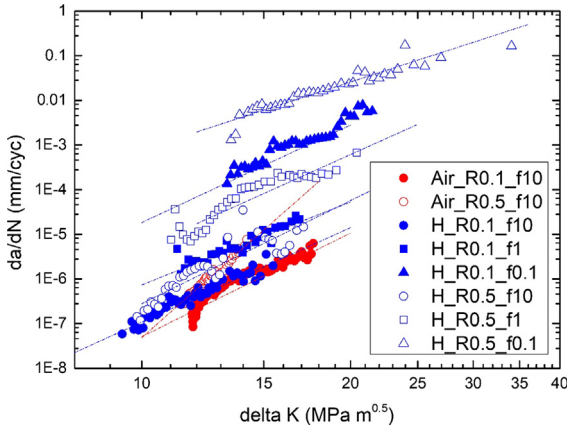

Fig. 4. Fatigue crack growth rate curves of Fe3wt%Si in the air and under different load ratio and frequency levels. The superposed dotted lines represent the linear Paris domain as obtained by using the coefficient reported in Table 2.

Table 2
Summary of the calculated Paris constants for the different resulting Fe-3%Si crack growth curves presented in Fig. 4.

Environment	R	f [Hz]	C	m
Air	0.1	10	1E−15	7.71
Air	0.5	10	1E−21	13.7
H	0.1	10	1E−14	7.03
H	0.1	1	5E−13	6.17
H	0.1	0.1	1E−12	7.26
H	0.5	10	6E−15	7.67
H	0.5	1	5E−13	6.98
H	0.5	0.1	7E−9	5.05

Table 3
Summary of the calculated Paris constants for the different resulting X70 pipeline steel crack growth curves reported in the plot in Fig. 5.

Environment	R	f [Hz]	C	m
Air	0.1	10	7E−10	3.12
H	0.1	10	6E−10	3.51
H	0.1	1	n.a.	n.a.
H	0.1	0.1	6E−07	2.25

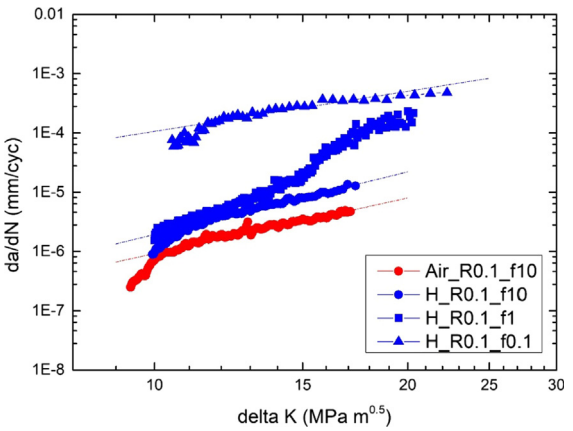

Fig. 5. Fatigue crack growth rate curves of X70 pipeline steel in the air and under different frequency levels (R = 0.1). The superposed dotted lines represent the linear Paris domain as obtained by using the coefficient reported in Table 3.

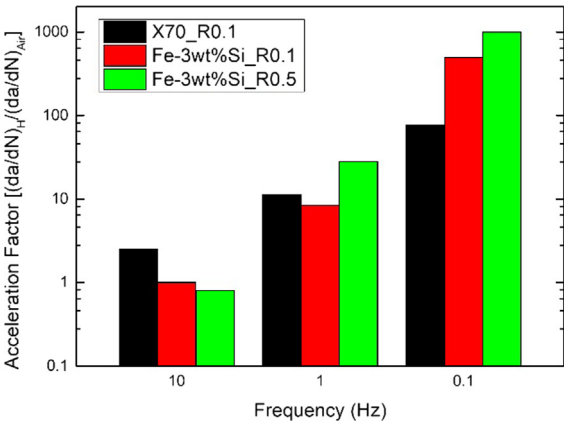

Fig. 6. Acceleration factors for the two investigated materials under the different tested conditions obtained for ΔK = 15 MPa.

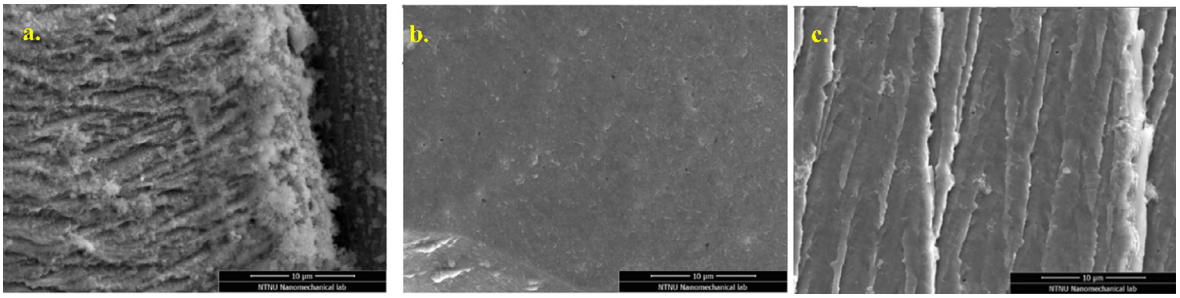

Fig. 7. Representative striation morphology in the three different fracture surface zones observed in the Fe-3%Si alloy: (a) Transgranular, (b) Intergranular, (c) Quasi Cleavage. All the images are from the in-situ electrochemically charged specimen tested at 0.1 Hz and R = 0.5. Crack growth is from up to down.

The acceleration factors for the materials tested and the different conditions is summarized in Fig. 6.

3.2. Fracture morphology characterization

All the tested Fe-3 wt%Si specimens have been subjected to fractography analysis. Three zones showing different main fracture morphologies have been identified: Transgranular (TG), Intergranular (IG) and "Quasi-Cleavage" (QC).

The in-depth analysis of the striation morphology exhibited in the different Fe-3%Si alloy with respect with the different fracture morphology has been already published by the authors in [7]. The transgranular zones are characterized by ductile striations aligned perpendicularly with the global crack growth testing direction. The intergranular zones features reveal grain-boundary-like surfaces/intergranular cleavage while "QC" zones features facets and smooth areas between striations, sometimes accompanied by river-marks. The analysis of the striation morphology revealed different characteristics appearance in the different microstructural zones and that they were dependent on the environmental conditions. For sake of reference, striations from TG zones are "dense and deep" (Fig. 7a) indicating a strong plastic deformation in front of the crack. The striations in the "QC" fracture zones are smoother (Fig. 7b) and with much smaller crests than in the QC zones. In the IG zones, no striations were observed (Fig. 7b).

In order to quantify the impact of the frequency on the mechanisms inherent to global FCG rate acceleration the quantitative statistical distribution of the different fracture morphologies have been made and already published by the authors [7]. Overall, the development and the relative ratio of the three fracture surface modes are strongly dependent on both test frequency and the ΔK level. As the ΔK level increases, the fracture mode changes from TG to "QC", while the fraction of IG type fracture always is relatively low, about 2–3% of the fracture surface, independently of the test conditions.

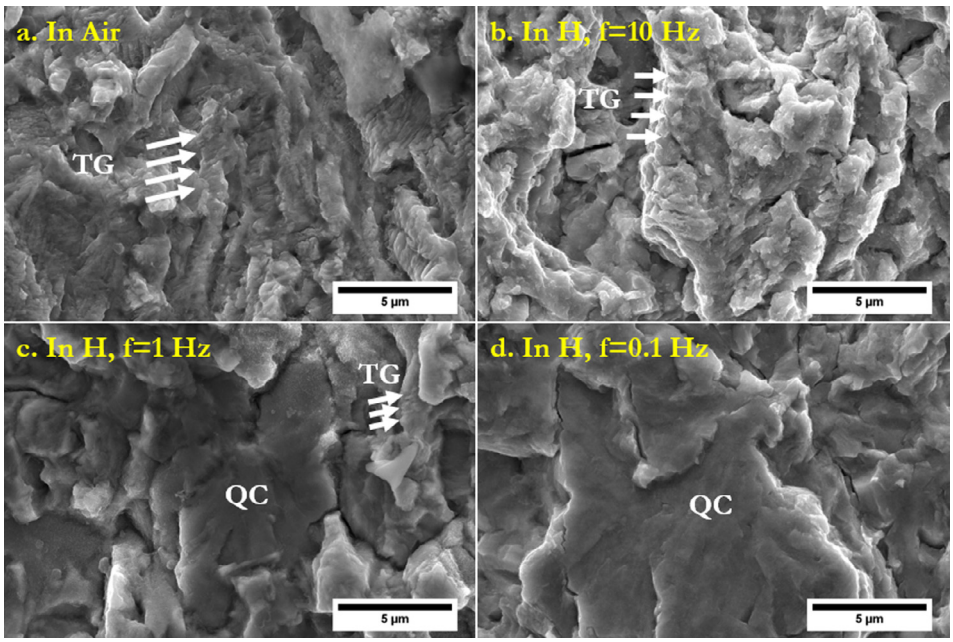

Fig. 8. Representative images of the different fractographic morphologies observed in the X70 steel for fixed ΔK = 15 MPa√m, global crack growth is from top to bottom: (a) in air; (b) In hydrogen, 10 Hz; (b) In hydrogen, 1 Hz; (b) In hydrogen, 0.1 Hz.

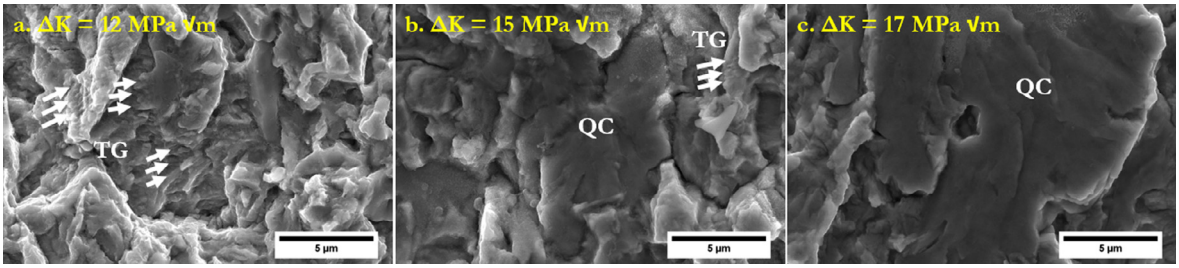

Fig. 9. Representative images of the different fractographic morphologies for X70 FCGR test in hydrogen at 1 Hz, global crack growth is from top to bottom: (a) ΔK = 12 MPa√m; (b) ΔK = 15 MPa√m; (c) ΔK = 17 MPa√m.

Analogous post-mortem analysis was performed on the X70 tested specimens. With reference to the plot in Fig. 5, the representative main fracture surface morphology for the different testing conditions and frequencies are reported in Fig. 8 for ΔK = 15 MPa√m.

Similarly, to what is observed for Fe-3 wt%Si, as the frequency is lowered and the global fatigue crack growth rate increases, the appearance of QC facets on the fracture surface increase. The same type of investigation has been performed for different ΔK levels for the test performed in hydrogen at 1 Hz, as shown in Fig. 9.

The overall fracture surface inspection reveals a shift of fracture morphology from transgranular to QC corresponding to an increase global FCGR as ΔK is increased.

3.3. Deformation structure

A thorough study of the dislocation structure and the mechanisms activated during the fatigue crack growth process in presence of hydrogen for the Fe-3%Si alloy has been already published [7,8]. The main findings led to the conclusion that the presence of hydrogen tend to hinder the formation of dislocation cells and tangles. In order to have a direct comparison between the deformation mechanisms in Fe-3%Si alloy and the X70 steel, similar investigation as the one presented in [7,8] have therefore been performed on X70 steel specimens.

Kernel Average Misorientation (KAM) (0–3°) on X70 steel specimens tested in air and in hydrogen condition (1 Hz) are presented in Fig. 10.

For the specimen exposed to hydrogen, at lower ΔK level (non-accelerated regime), a relatively large plastic zone can be observed, giving dislocation shielding and crack blunting effects and consequently TG fracture feature. At higher ΔK level (accelerated regime), an obviously reduced plastic zone is presented, showing good agreement with the previous results in the model Fe-3 wt%Si alloy [7–9].

Electron Channeling Contrast Imaging (ECCI) have been performed on the X70 steel both in air and H-exposed (1 Hz test which showed the transition from non accelerated to accelerated regime) specimen. In Fig. 11, the overall deformation structure developed in the crack wake is shown.

In air, dislocations form walls and tangles below the fracture surface at lower ΔK levels. When the ΔK level gets higher, the dislocations start to form cells, indicating a larger plastic deformation. In the hydrogen exposed specimen, the dislocation structure looks similar to the one in air at lower ΔK levels (non-accelerated regime). At higher ΔK levels (accelerated regime), dislocation cells are also visible in the hydrogen case, but only in a much more reduced area. Higher magnification of the region of interest presented in Fig. 11 are reported in Fig. 12.

High-magnification detailed dislocation structure images show a really similar dislocation arrangement in the non-accelerated regime (Fig. 12a.vs. Fig. 12b), but a lower dislocation density appears in the hydrogen exposed case. On the other hand, at higher ΔK levels, i.e. in the hydrogen accelerated regime, both the deformation structure in air and hydrogen show the formation of dislocation cells. Despite the high magnification images do not reveal a clear difference between the single cells (Fig. 12b. vs. Fig. 12d), the extension of the deformation zone characterized by these cells seems to be less in the case of hydrogen, as it can be seen from the images in Fig. 10 and Fig. 11.

4. Discussion

It is well known and documented that the presence of hydrogen can change the fatigue fracture mode from ductile striations to cleavage-like, often referred to as quasi-cleavage, in iron base alloys and steels [7,10–20]. Vehoff [21] observed similar structures in Fe-2.6%Si single crystals under gaseous H_2 environment. In order to explain the sharp cleavage fracture structure, they postulated that crack grows stably in a stepwise micro-cleavage manner. Same features were also observed in a Fe-Si alloy by Takahashi [22], while Shinko [23] investigated HA-FCGR in commercially pure iron in terms of hydrogen gas pressure. HA-FCGR in low carbon steels was studied by Nishikawa [11], Matsuoka [24] and Yamabe [25] while Ronevich [26,27] investigated ferritic-pearlitic pipeline steels, all performing FCG tests in H_2 gaseous environments. Fassina [28] investigated the fatigue properties variation on pipeline steels, i.e. F22 and X65, due to hydrogen electrochemical pre-charging. The impact of hydrogen on the fatigue crack growth rates of different materials is also strongly dependent on the testing parameters utilized: frequency, temperature, load ratio, cycle shapes are

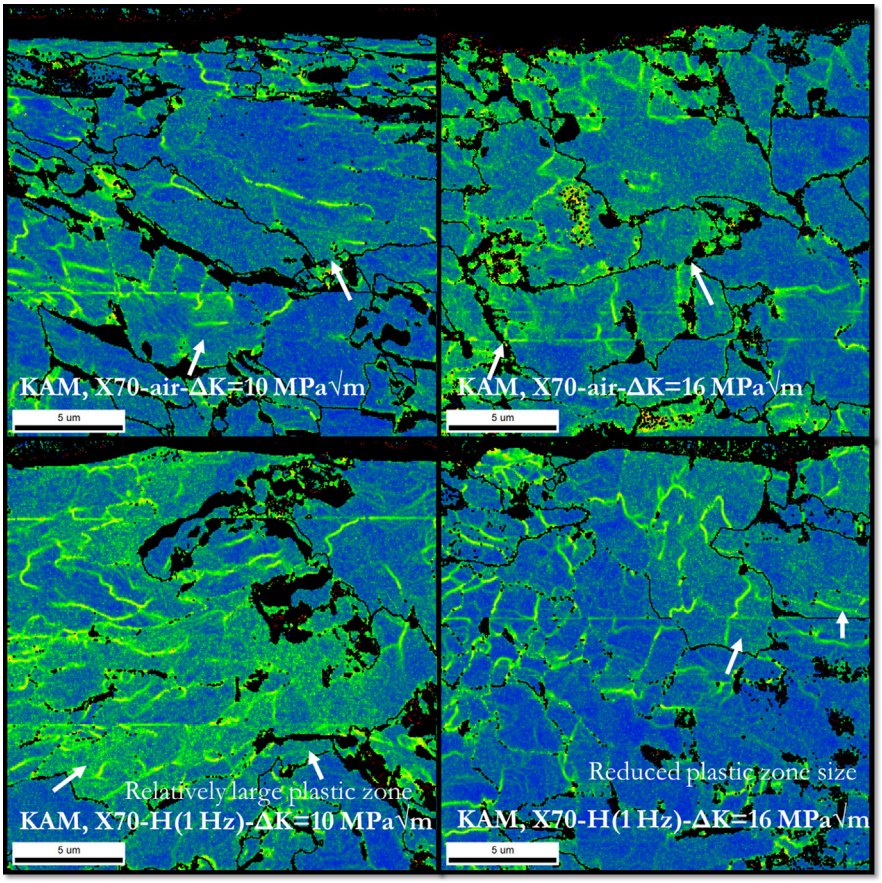

Fig. 10. Kernel Average misorientation maps obtained on post-mortem analysis of the X70 steel. Material, frequency and ΔK level are indicated in the figure. Global FCG direction from left to right.

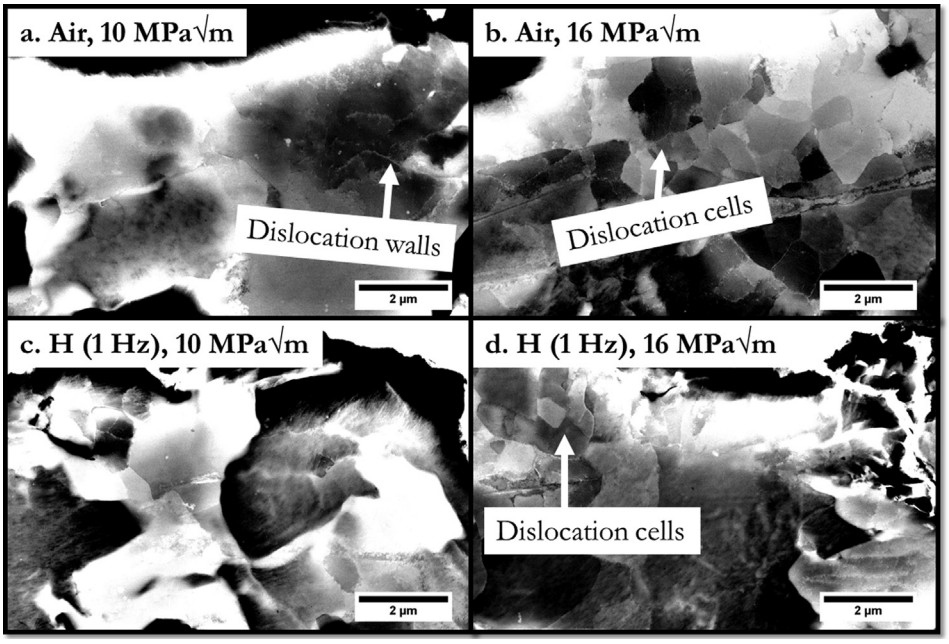

Fig. 11. Dislocation structure developed in the crack wake for the X70 steel. Environment conditions, frequency and ΔK levels are indicated in the figure. The global fatigue crack growth direction if from the left to the right.

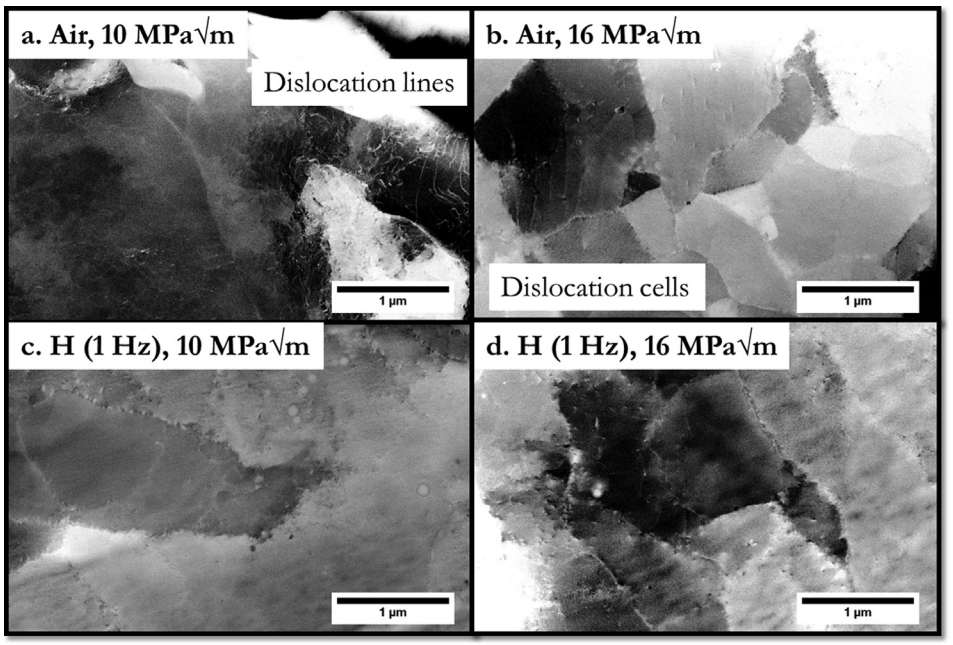

Fig. 12. Higher magnification of the regions of interest in X70 steel presented in Fig. 11. The global fatigue crack growth direction if from the left to the right.

the among the most studied and reported ones [14,19,20,25,29].

In this study, the effect of hydrogen on fatigue crack growth rate of two ferrous alloys, has been revealed in line with the previous studies on the topic: qualitatively the global fatigue crack growth rate increases for both materials when hydrogen is present, and the average acceleration factor strongly depends on the test frequency. The lower the frequency, the stronger the acceleration induced by the hydrogen presence, confirming the time-dependent nature of HA-FCG. For the Fe-3 wt%Si the hydrogen induced fatigue crack growth rate enhancement is also stronger as the applied load ratio is increased.

Post-mortem surface characterization clearly shows how the global fatigue crack growth rate enhancement strongly relates to the shift in mechanisms observed on the fracture surface: crack growth acceleration corresponds to the appearance of QC facets over transgranular ductile fracture morphology. Another specific feature of the fracture surface investigation is the low presence of IG features in Fe-3 wt%Si and the totally absence of IG in the X70 pipeline steel. This is in accordance with the results of Hajilou et al. [30] who performed microcantilever bending test on the same Fe-3wt%Si alloy under in-situ electrochemical H-charging conditions. Hajilou et al. [30] showed that grain boundaries are not more sensitive than the grain for propagation of the crack under the influence of the hydrogen, and the crack propagation of the highest stress concentration path. This is indicative toward a relatively low propensity of the material to intergranular cracking, despite the inherent difference between fatigue ductile crack growth mechanisms (even in the case of cracking along microstructural interface) from the monotonic deformation-induced cracking. According to McMahon [31], the H-assisted IG fracture in steels strongly depends strongly on the impurities segregated to the GBs. However, most H-assisted failure events relates to hydrogen diffusing into the region of high hydrostatic stress. Furthermore, the brittle cyclic cleavage fracture observed in the Fe-3 wt%Si in this study (Fig. 7c) are practically identical to the ones reported by Shinko [23] as representative of the striation mechanisms active in the accelerated regime. They explained such topography in terms of crack tip sharpening and hydrogen-enhanced decohesion process.

The Fe-3 wt%Si material is heat-treated at high temperature followed by water quenching so that little grain boundary segregation is expected which decreases the possibility that IG fracture occur. However, even if the two materials qualitatively show the same frequency-dependent general behaviour in presence of hydrogen, there are important quantitative differences between the HA-FCG behaviour of Fe-3 wt%Si and the X70 pipeline steel. The first difference relates to the magnitude of the hydrogen-induced enhancement: for the tests at 0.1 Hz and R = 0.1, the Fe-3 wt%Si features a crack growth acceleration of about 500 times while the X70 steel revealed an acceleration factor of about 70. This level of crack growth rate enhancement due to hydrogen charging is in the same order of magnitude as the one recorded on X65 by Fassina [28] (about 50 times for electrochemically pre-charged hydrogen) and by Cialone [32] (Stage II growth in X42 over 100 times faster when exposed in 6.9 MPa gaseous H2 compared to Nitrogen/inert environment). Second, while the Fe-3 wt%Si revealed a shift of the whole crack growth curves with decreasing frequency, the X70 steel for the test at 0.1 Hz showed a clear transition towards accelerated crack growth with increasing ΔK. This behaviour is in accordance with Matsuoka [24] on Cr-Mo steel and by Ogawa [17,33] and Shinko [23] who investigated the HA-FCG behavior of pure iron under different H_2 pressure levels. One reason behind the increased magnitude of the embrittlement sensitivity in Fe-3%Si resides in the Silicon content of the alloy. As shown by Nakasato [34], the addition of Si tends to strongly favour cleavage cracking which, in turn will infer a strong acceleration in the global fatigue crack growth rate.

When analysing the deformation mechanisms through EBSD and ECCI investigations, the comparison between the dislocations structure developed in the crack wake between the Fe-3%Si alloy [7–9,18] and the X70 steel revealed the same behaviour, at least from a qualitatively point of view. In hydrogen, the fatigue crack is producing a reduced plastic zone with an accelerated crack growth rate in comparison with the air case when subjected to the same mechanical/loading conditions. The plasticity accumulated beneath the fracture surface is much larger for the specimens tested in air, i.e. the misorientation profile recorded features higher values, than the one measured in the specimens tested in hydrogen, and this is qualitatively the same behaviour both for the Fe-3%Si alloy and the X70 steel investigated in this study.

On the other hand, some differences are observable with respect to the eventual variations in air and in hydrogen in the dislocation arrangement for the X70 steel and the Fe-3%Si alloy. For the Fe-3%Si, dislocations arrange in cells, tangles and walls when tested in air while nearly no cells are detectable in the case of the specimen tested in hydrogen [7–9,18]. For the case of X70, dislocations cells are always observed both in air and hydrogen with the difference residing in the size of the dislocation cell evolution region. The results on X70 are in good agreement with the observations presented on HA-FCG study on pure Fe [17,23,33,35] in which dislocations cells are always present, even in the hydrogen accelerated regime. This also confirms that no significant differences in the hydrogen affected deformation activities between pure iron and ferritic-pearlitic microstructure, not only in the case of H_2 pressurized charging [36,37], but also in the case of electrochemical charging.

There are two points to be noted. The first one is that no focus has been pointed toward the evaluation of the influence of the electro-chemical parameters in the present study. It can be argued that the electro-chemical conditions, and in particular the electro-chemical potential chosen in this study, i.e. $-1400\,mV_{SCE}$, are particularly stringent when it comes to determining hydrogen saturation at the crack tip. Such choice may, in turn, affect the different material sensitivity to HA-FCGR, particularly with respect to the frequency effect. This topic is one of the most interesting candidates for future work by the present group. The second point concern the fact that the reference testing and evaluation with respect to the deformation evolutions are made in air, which could be, to any extent, be considered an active environment on which even hydrogen could be absorbed [29,38]. These topics will need to be addressed in future work.

5. Conclusions and further work

The influence of hydrogen on the fatigue crack growth behavior in a Fe-3wt%Si alloy and a pearlitic-ferritic X70 pipeline steel under in-situ electro-chemical H charging condition was studied. The fracture surface morphologies were investigated and the effect of test frequency on the fracture mode transition was discussed with respect to the analogies and the differences in FCGR for the two materials.

The following conclusions are drawn:

- In situ H-charging enhanced the FCGR for the Fe3%Si material up to 1000 times and up to 76 times for the X70 pipeline steel compared to testing in air.
- The results clearly show the time-dependent nature of the H-induced degradation interaction: a lower frequency leads to more severe degradation of the FCG process.
- Post-mortem fractography clearly showed a shift in crack growth mechanisms: the FCG mode of both Fe-3wt%Si alloy and X70 steel changed from transgranular to Quasi-cleavage; IG type fracture was really limited in Fe-3 wt%Si and absent in X70, indicating that the grain boundaries are not preferential paths for crack propagation.
- The maximum acceleration factor obtained for Fe-3wt%Si was one order of magnitude larger than for the X70 steel, indicating a strong influence of the difference in microstructure (grain sizes and phases) with respect to HA-FCGR susceptibility.
- The observation of the dislocation structure developed in the crack wake indicates no significant differences in the hydrogen affected deformation activities between pure iron and ferritic-pearlitic microstructure, also in the case of electrochemical charged hydrogen.

Different charging methods and more advanced characterization methods may be applied to study the fundamental mechanism of the H-assisted cracking phenomena. A study of the effect of different electrochemical charging parameters on the degree of hydrogen affect fatigue crack growth in connection to the deformation behaviour in the crack wake will be a subject of future work.

Acknowledgments

This work was financially supported by the Research Council of Norway (Petromaks2 Program, Project No. 244068/E30, HyFLEx). The authors also thank Ing. Tore Andre Kristensen for the help in the experimental challenges.

References

[1] Suresh S, Ritchie R. On the influence of environment on the load ratio dependence of fatigue thresholds in pressure vessel steel. Eng Fract Mech 1983;18(4):785–800.
[2] Colombo C, et al. Fatigue behavior of hydrogen pre-charged low alloy Cr–Mo steel. Int J Fatigue 2016;83:2–9.
[3] Ritchie RO. Mechanisms of fatigue-crack propagation in ductile and brittle solids. Int J Fract 1999;100(1):55–83.
[4] Somerday B, et al. Elucidating the variables affecting accelerated fatigue crack growth of steels in hydrogen gas with low oxygen concentrations. Acta Mater 2013;61(16):6153–70.

[5] Alvaro A, et al. Fatigue properties of a 420 MPa structural steel at low temperature. The 25th international ocean and polar engineering conference. 2015: Kona, Big Island, Hawaii, USA. 2015. p. 331–7.
[6] Paris P, Erdogan F. A critical analysis of crack propagation laws. J Basic Eng 1963;85(4):528–33.
[7] Wan D, et al. Hydrogen-enhanced fatigue crack growth behaviors in a ferritic Fe-3wt% Si steel studied by fractography and dislocation structure analysis. Int J Hydrogen Energy 2019.
[8] Wan D, et al. Hydrogen-enhanced fatigue crack growth in a single-edge notched tensile specimen under in-situ hydrogen charging inside an environmental scanning electron microscope. Acta Mater 2019;170:87–99.
[9] Alvaro A, et al. Hydrogen enhanced fatigue crack growth rates in a ferritic Fe-3wt%Si Alloy. European Conference of Fracture. Belgrade: Elsevier; 2018.
[10] Marrow T, Cotterill P, King J. Temperature effects on the mechanism of time independent hydrogen assisted fatigue crack propagation in steels. Acta Metall Mater 1992;40(8):2059–68.
[11] Nishikawa H-A, Oda Y, Noguchi H. Investigation of the mechanism for brittle-striation formation in low carbon steel fatigued in hydrogen gas. J Solid Mech Mater Eng 2011;5(8):370–85.
[12] Murakami Y, et al. Hydrogen embrittlement mechanism in fatigue of austenitic stainless steels. Metall Mater Trans A 2008;39(6):1327.
[13] Murakami Y, Matsuoka S. Effect of hydrogen on fatigue crack growth of metals. Eng Fract Mech 2010;77(11):1926–40.
[14] Hénaff G, Odemer G, Tonneau-Morel A. Environmentally-assisted fatigue crack growth mechanisms in advanced materials for aerospace applications. Int J Fatigue 2007;29(9–11):1927–40.
[15] Sun Z, et al. Fatigue crack growth under high pressure of gaseous hydrogen in a 15–5PH martensitic stainless steel: influence of pressure and loading frequency. Metall Mater Trans A 2013;44(3):1320–30.
[16] Yamabe J, et al. Hydrogen trapping and fatigue crack growth property of low-carbon steel in hydrogen-gas environment. Int J Fatigue 2017;102:202–13.
[17] Ogawa Y, et al. Multi-scale observation of hydrogen-induced, localized plastic deformation in fatigue-crack propagation in a pure iron. Scr Mater 2017;140:13–7.
[18] Wan D, et al. Hydrogen-assisted fatigue crack growth in ferritic steels–a fractographic study. MATEC Web of Conferences. EDP Sciences; 2018.
[19] Matsunaga H, et al. Hydrogen-enhanced fatigue crack growth in steels and its frequency dependence. Phil Trans R Soc A 2017;375(2098):20160412.
[20] Matsuoka S, et al. Peculiar temperature dependence of hydrogen-enhanced fatigue crack growth of low-carbon steel in gaseous hydrogen. Scr Mater 2018;154:101–5.
[21] Vehoff H, Rothe W. Gaseous hydrogen embrittlement in FeSi-and Ni-single crystals. Perspectives in hydrogen in metals. Elsevier; 1986. p. 647–59.
[22] Takahashi Y, et al. An intrinsic effect of hydrogen on cyclic slip deformation around a {1 1 0} fatigue crack in Fe–3.2 wt% Si alloy. Acta Mater 2010;58(6):1972–81.
[23] Shinko T, et al. Hydrogen-affected fatigue crack propagation at various loading frequencies and gaseous hydrogen pressures in commercially pure iron. Int J Fatigue 2019;121:197–207.
[24] Matsuoka S, et al. Influence of hydrogen and frequency on fatigue crack growth behavior of Cr-Mo steel. Int J Fract 2011;168(1):101–12.
[25] Yamabe J, et al. Effects of hydrogen pressure, test frequency and test temperature on fatigue crack growth properties of low-carbon steel in gaseous hydrogen. Procedia Struct Integr 2016;2:525–32.
[26] Ronevich JA et al. Measurement of fatigue crack growth relationships for steel pipeline welds in high-pressure hydrogen gas. Livermore, CA (United States): Sandia National Lab. (SNL-CA); 2014.
[27] Ronevich JA, Somerday BP, San Marchi CW. Effects of microstructure banding on hydrogen assisted fatigue crack growth in X65 pipeline steels. Int J Fatigue 2016;82:497–504.
[28] Fassina P, et al. Influence of hydrogen and low temperature on mechanical behaviour of two pipeline steels. Eng Fract Mech 2012;81:43–55.
[29] Petit J, Henaff G, Sarrazin-Baudoux C. Environmentally assisted fatigue in the gaseous atmosphere. Comprehen Struct Integr 2003;6:211–80.
[30] Hajilou T, et al. In situ electrochemical microcantilever bending test: a new insight into hydrogen enhanced cracking. Scr Mater 2017;132:17–21.
[31] McMahon CJ. Hydrogen-induced intergranular fracture of steels. Eng Fract Mech 2001;68(6):773–88.
[32] Cialone H, Holbrook J. Effects of gaseous hydrogen on fatigue crack growth in pipeline steel. Metall Trans A 1985;16(1):115–22.
[33] Ogawa Y, et al. The role of intergranular fracture on hydrogen-assisted fatigue crack propagation in pure iron at a low stress intensity range. Mater Sci Eng A 2018.
[34] Nakasato F, Bernstein I. Crystallographic and fractographic studies of hydrogen-induced cracking in purified iron and iron-silicon alloys. Metall Trans A 1978;9(9):1317–26.
[35] Birenis D, et al. Interpretation of hydrogen-assisted fatigue crack propagation in BCC iron based on dislocation structure evolution around the crack wake. Acta Mater 2018;156:245–53.
[36] Drexler ES, et al. Fatigue crack growth rates of API X70 pipeline steel in a pressurized hydrogen gas environment. Fatigue Fract Eng Mater Struct 2014;37(5):517–25.
[37] Bilotta G, et al. Environmentally-assisted fatigue crack growth in ARMCO iron under high pressure of gaseous hydrogen. International hydrogen conference (IHC 2016): materials performance in hydrogen environments. ASME Press; 2017.
[38] Henaff G, Petit J, Bouchet B. Environmental influence on the near-threshold fatigue crack propagation behaviour of a high-strength steel. Int J Fatigue 1992;14(4):211–8.